LBL-19464
Preprint c.2

# Lawrence Berkeley Laboratory

UNIVERSITY OF CALIFORNIA

RECEIVED
LAWRENCE
BERKELEY LABORATORY
OCT 9 1985
LIBRARY AND
DOCUMENTS SECTION

## Materials & Molecular Research Division

To be submitted for publication

IN-SITU OBSERVATIONS OF PARTIAL DISLOCATION CLIMB IN $Ni_3Al$

P. Veyssière and K.H. Westmacott

August 1985

TWO-WEEK LOAN COPY
This is a Library Circulating Copy
which may be borrowed for two weeks

LBL-19464 c.2

Prepared for the U.S. Department of Energy under Contract DE-AC03-76SF00098

## DISCLAIMER

This document was prepared as an account of work sponsored by the United States Government. While this document is believed to contain correct information, neither the United States Government nor any agency thereof, nor the Regents of the University of California, nor any of their employees, makes any warranty, express or implied, or assumes any legal responsibility for the accuracy, completeness, or usefulness of any information, apparatus, product, or process disclosed, or represents that its use would not infringe privately owned rights. Reference herein to any specific commercial product, process, or service by its trade name, trademark, manufacturer, or otherwise, does not necessarily constitute or imply its endorsement, recommendation, or favoring by the United States Government or any agency thereof, or the Regents of the University of California. The views and opinions of authors expressed herein do not necessarily state or reflect those of the United States Government or any agency thereof or the Regents of the University of California.

# In-situ Observations of Partial Dislocation Climb in $Ni_3Al$

P. Veyssière* and K.H. Westmacott

National Center for Electron Microscopy
Materials and Molecular Research Division
University of California
Lawrence Berkeley Laboratory,
Berkeley, CA 94720
U.S.A.

*Permanent Address: Laboratoire de Métallurgie Physique, Faculté des Sciences, 40, Avenue du Recteur Pineau, 86022 Poitiers, France

## Abstract

Changes in the configuration of screw and mixed dislocations in $Ni_3Al$ have been monitored continuously during annealing in the hot stage of a high voltage electron microscope. Differences in the configurations were observed depending on whether the experiments were performed below or above the threshold voltage $V_t$ for displacement damage.

Below $V_t$, initially straight dislocations in or close to screw orientation slowly increased their length and segmented into non-screw components during heating at 750° C. This behaviour is attributed to a resulting reduction in energy as the newly oriented segments climb dissociate in a more favorable plane where the APB energy is lower than the initial {001} glide dissociation plane.

Above $V_t$, radiation-produced interstitials induce asymmetrical climb of the ½<110> superpartial screw dislocations during irradiation at 650° C. One partial remains essentially unchanged as the other climbs into a helical configuration in a direction away from the position of the original screw dislocation. Energy balance considerations show that the single rather than double helix configuration will be favoured if the associated APB energy is

low. It is suggested that the low energy APB is produced when helix turns are formed by the condensation of interstitial nickel atoms in an off-stoichiometric layer. The occasional observation of residual displacement fringe contrast supports this view.

## 1. Introduction

In deformed $Ni_3Al$, dislocations are predominantly observed to be dissociated into two partials either with collinear ½<110> Burgers vector (BV) separated by an antiphase boundary (APB) or with 1/3<112> BV's bordering a superlattice intrinsic stacking fault (SISF) (for a review, see Pope and Ezz 1984). However, the former dissociation mode prevails during deformation whereas the latter can be regarded as a by-product of deformation which does not control the intrinsic mobility of dislocations (Veyssière, Beauchamp and Douin 1985). Provided the dislocation line lies within about 25° of the screw orientation, dissociation into two ½<110> BV's occurs by glide on {001}. The segments with more pronounced edge character exhibit the unusual property of being dissociated by climb if the temperature of the deformation test is high enough to allow for atomic interchange between the partials (Veyssière, Guan and Rabier 1984, Veyssière 1984). Whereas examples of mixed dislocations having undergone diffusional splitting are seldom at 350 °C, they are systematically encountered above 650-700° C. Nevertheless, the dislocation microstructure at 650° C still indicates that screw dislocations remain the most sessile components. At 800° C, however, the situation is reversed since the shape of the dislocations lying in the {001} glide planes now attests to a lesser mobility of the non-screw parts. So far, the well-known increase of strength which occurs in $Ni_3Al$ up to 700 °C was thought to result only from a cross-slip locking mechanism (Kear

and Wilsdorf 1962, Takeuchi and Kuramoto 1973, Paidar, Pope and Vitek 1984). It is likely however, that the situation is more complex (Veyssière, 1984, Huis in't Veld, Boom, Bronsveld and De Hosson 1985, Paidar 1985), indeed it is speculated that the rate-controlling role of cross-slip at room and intermediate temperatures might be carried over to higher temperatures by the formation of climb locks which give the materials its largest strength. Thus, it appears important to characterize and understand climb dissociation in the $L1_2$ structure in view of its possible rate-controlling role during deformation.

The present investigation was initiated to help elucidate the process by which a dislocation resulting from deformation at moderate temperature evolves from a glide to a climb dissociated configuration when annealed in-situ in the electron microscope at elevated temperatures. In order to eliminate possible artifacts resulting from the interaction of the dislocations with the free surfaces, reasonably thick samples were examined using a high voltage instrument. The present paper reports on observations carried out in $Ni_3Al$ for which drastically different dislocation responses to annealing have been detected depending upon whether climb is induced by radiation produced interstitials or by thermal vacancies.

## 2. Experimental

Polycrystalline parallelepipeds were deformed in compression under an argon atmosphere at different temperatures ranging from room temperature to 800°C. The strain-rate was $2 \times 10^{-5}$ $s^{-1}$ and deformation was stopped as soon as a deviation from linearity on the stress-strain curve was detected. This provided a moderate density of dislocations in the samples with limited dislocations reactions. The samples were then sliced at 45° from the compression axis in order to maximize the chances to obtain sections containing a glide

direction if not a glide system. The slices (0.5 mm thick) were mechanically thinned to 0.1 mm and their faces carefully polished with alumina prior to electropolishing (Veyssière et. al. 1984).

The samples were selected such that they would exhibit large arrays of long screw dislocations. They were subsequently examined in a Kratos EM 1500 high voltage electron microscope operating between 300 kV and 1.5 MV using a double-tilt heating stage capable of raising the temperature of the sample to 850°C. The specimen chamber vacuum varied with the holder temperature, and was initially in the range 3-7 x $10^{-7}$ mPa. Subsequent modifications to the system improved the minimum pressure to 7 x $10^{-8}$ mPa. The annealing sequences were continuously recorded on a video tape via a video camera mounted below the column. Additional analyses of the samples were performed with a JEOL 200 CX and a Siemens 102 operating at 200 kV and 100 kV respectively.

## 3. Thermal Dislocation Climb

### 3.1 Observations

Preliminary experiments established the threshold voltage for displacement $V_t$ in $Ni_3Al$ to be 320 $\pm$ 10 kV. The procedure for determining $V_t$ consisted of submitting an area containing loops formed by irradiation at 615°C to further irradiation with a fully focussed condenser lens and observing the voltage at which they would continue growing within a time of 30 minutes.

At operating voltages below $V_t$, the evolution of the dislocation substructure depends only on the specimen temperature, with significant changes occurring at 750°C over the course of an hour. Since the object was to observe the influence of climb dissociation on dislocations, the experiments were generally conducted on individual screw dislocations. Ideally, the transition from a glide to a climb-split mixed or edge segment would be the most relevant

phenomenon to look for. However, the deformation microstructure introduces specific constraints and prevents this case from being studied. Indeed, at temperatures where lengths with such orientations are created to a sufficiently large extent, they are already dissociated by climb, thus moderate evolution, if any, would be expected during subsequent in-situ annealing experiments. When dislocations are not climb dissociated, i.e. at low and moderate temperatures, they appear in the form of bowed mixed segments within a very large density of long nearly screw dislocations, but the mixed segments are generally too short to provide significant information.

A sequence of micrographs illustrating evolution of the dislocation microstructure during annealing at 750°C is presented in Fig. 1. The thin foil, approximately parallel to (111), initially contained two families of long screw dislocations with $[1\bar{1}0]$ and $[\bar{1}01]$ slip directions together with many short screw segments inclined to the foil. Typically, the dislocations evolve in three different ways. First, unavoidable thin foil effects modify the structure: dislocations rotate under the attraction of image forces and while some may leave the foil completely, most remain in steeply inclined configurations ($\alpha$); this results in a drastic reduction of the dislocation density. Secondly, when they belong to dipoles which are wholly contained in the foil, the closing mixed segments (i.e. the dislocation(s) that join a dipole at its end(s)) undergo viscous glide under the effect of the back force that tends to reduce the total line energy. The motion of the screws one toward the other is also detectable and occurs at a rate comparable to that of the closing segment ($\beta$). This points to the fact that screw dislocations are rather sessile in $Ni_3Al$ up to 750°C, but the reason for this is related to the kinking process described below rather than any process connected to

cross slip. Thirdly, the remaining screw dislocations turn progressively into kinked ones with mixed parts ($\gamma$). Only the last process will be detailed here since this transformation of a straight screw line into a succession of segments with mixed character results in a net increase in line length. In the absence of an applied stress this is only possible if the dislocation energy per unit length is sharply reduced for some particular orientation of the line compared to that of the screw orientation.

The samples annealed in-situ were re-examined at room temperature in conventional voltage microscopes. Stereomicroscopy revealed complex features, Figs. 2 and 3, details of which are summarized in the accompanying stereographic projections. Kinking occurs in such a way that the segments may deviate up to 50° from the initial screw orientation. Their motion takes place such that the final segmented dislocation does not belong to a single plane. Since two consecutive segments may occasionaly define a plane which does not contain their Burgers vector, in these cases the evolution of the dislocation lines must have involved local climb. On the other hand, it is interesting to study which glide planes are locally activated; these correspond to planes containing both the Burgers vector and two consecutive segments. Apart from one case where the {111} low temperature easy glide plane (LTGP) in $Ni_3Al$ has been identified, the high temperature easy glide plane {001} (HTGP) together with the unexpected {110} plane are observed most commonly, the latter being the most frequent. This is the first time that evidence for {110} slip in $Ni_3Al$ is reported, but since it has been activated under the driving force of climbing neighbouring segments, the present observations cannot be construed as evidence for macroscopic {110} glide of $Ni_3Al$.

3.2 Discussion

Apart from dislocation line instabilities resulting from negative line tension for some glide orientations in {001} planes, there are no sharp cusps expected at dislocations with <110> BVs expanding in crystallographic planes other than {001} (J. Douin, P. Veyssière and P. Beauchamp 1985: unpublished results). Therefore, the observed segmentation of initially screw dislocations cannot result from the fact that, because annealing causes their mobility to increase, they may then adopt lower energy kinked configurations solely under the dictates of anisotropy. Also, since a glide APB on {001} has the lowest energy amongst all potential glide APB's (Flinn 1960, Yamaguchi, Paidar, Pope and Vitek 1982), and the dislocations already satisfy this condition, thermal kinking will not be dictated by glide considerations. Rather, segmentation of the screw dislocations is likely to result from a large reduction in energy per unit length due to dissociation by climb. Such an effect has already been reported to occur on deformation dislocations loops in $Ni_3Al$ expanding in their {001} glide plane (Veyssière 1984). However, in this study, dislocation lines along near edge <013>, <012> and <011> orientations were observed to exhibit climb dissociation whereas lines lying within $\pm$ 20° of screw character glide dissociated on {001} . In contrast, thermal kinking favours those line orientations within the $\pm$ (20°-40°) of screw character which on {001} glide loops are usually unstable but remain straight (Veyssière 1984). In the present context, the differences between apparent line stabilities in $Ni_3Al$ depending upon whether it was strained or annealed at elevated temperatures might simply result from the fact that, during annealing, there exists a large component of climb in the motion of the total superdislocation (BV=<110>) as mentioned in 3.1, which modifies the condition for line stability. In fact, since the stress acting

on the whole dislocation clearly varies according to the local edge character of the line, the conditions which govern the eventual shape of a dislocation during annealing cannot compare to those established during glide where there is only a constant shear stress acting regardless of character. As a concluding remark on thermal kinking, it will be pointed out that, this process occurs in such a way that a line orientation consistent with climb dissociation occurring on {013} planes (others are not excluded) is resolved at the end of the annealing sequence; the initially screw dislocations deform and increase their length, in a manner which involves not only climb but also glide of the superdislocations in {001}, {111} and locally in {110}. Thus, it appears that the manifestations of climb dissociation sought in this study have been obtained only as part of a more complex reorganization of the dislocation microstructure. At present, final conclusions cannot be drawn but further experiments in progress may clarify the situation.

## 4. Radiation-Induced Climb of Dislocations

### 4.1 Observations

All the observations reported in this section have been carried out above $V_t$ at temperatures between 25 and 800°C.

The formation rate of secondary defects depends both on the voltage and on the temperature; it is a maximum between 630°C and 680°C at 1500kV. The upper temperature for loop formation is approximately 700°C as a result of the increasing probability of recombination of radiation-produced interstitials with thermal vacancies. Above 750°C, loops as well as helical dislocations created by irradiation at lower temperatures tend to shrink and often disappear attesting to a net permanent flux of vacancies precipitating onto them. The kinetics of formation as well as the extrinsic nature of the faulted and

unfaulted loops resulting from irradiation at 650 kV has already been determined by Liu and Mitchell (1982); these experimental results are reproducible at any voltage above 400 kV. It was also observed in the present study that the loop nucleation rate in the matrix was sensitively dependent on the specimen chamber vacuum. In later experiments performed in a vacuum of 7-12 x $10^{-8}$ mPa, loop nucleation at higher temperatures was almost suppressed, providing further confirmation of the importance of residual gas in the specimen on secondary defect formation (Glowinski 1976).

As far as climb of prexisting screw dislocations is concerned no effect is apparent up to 600° C even after an irradiation time of ½ hour, whereas numerous individual loops may form in the matrix. At 630°C, the evolution is slow but it can be accelerated by fully focussing the condenser lens. 650° C is the temperature at which the observation conditions are optimized. Climb over distances of the order of 100 nm then occurs in a matter of seconds, and it can be slowed or stopped and frozen-in at any time by defocussing the beam. A montage showing a typical distribution of Frank loops, rhombus loops, and helices in an irradiated region is given in Fig. 4.

Contrary to what happens at individual loops formed in the matrix, climb at screw dislocations always occurs by nucleation and growth of ½<110> APB helical turns. We have not observed any example of growth events where turns with 1/3<112>, 1/6<112> or crystallographically equivalent displacement vectors are involved. Perfect <110> dislocation helix turns were not observed either. The climb sequence starts by nucleation of small triangles which appear only on the region of the dislocation under irradiation. These do not grow in size below 630°C, but their density increases as the irradiation proceeds. Above 650°C, giant helix turns may grow from these triangles (Fig. 5) with no tendency

for the pitch to change. It is noteworthy that only one of the $\frac{1}{2}\langle 110\rangle$ partials generally climbs into a triangle or a helix turn, in other words, once climb is nucleated on one partial, the other remains in screw orientation (Figs. 4 and 5). There is occasional evidence that the role played by each partial may be reversed on the same dislocation from a given pitch to its neighbour, as illustrated in Fig. 6.

A stereomicroscopy determination of the line orientations of the segmented helix turns with $\frac{1}{2}[1\bar{1}0]$ total BV has been performed; the results are summarized in Table 1. These can be described as a periodic sequence of orientations ... A B C D A . . ., such that the segments BCD belong to the $(1\bar{1}0)$ plane. Also listed in Table 1, are the planes containing two consecutive segments; these are just indicative of one possible APB combination. Because the structure factors of the superlattice reflections are not appropriate to allow for detailed APB imaging in $Ni_3Al$, the geometrical details of the associated APB's could not be determined. Nevertheless, the topography of the APB bounded by the superpartials can be visualized readily with a model such as that depicted in Fig. 7 which shows that the climb configuration can adopt a specific APB plane only during the later stages of asymmetrical growth. Figure 8 shows a climb sequence of a widely extended inclined helix which confirms that the turns appear to be constrained to be in the $(1\bar{1}0)$ plane normal to the BV.

Although these experiments were conducted almost exclusively on screw dislocations, there were instances where irradiation-induced climb of mixed segments was identified. In these, the elementary steps which transform the glide dissociated configuration into a climb one have not been elucidated yet. However, it has been repeatedly observed that after some incubation time, whereas one partial remains located almost at the same place, its companion moves

away undergoing extensive climb (Fig. 9). Surface effects seemed to play a dominant role in the examples we have observed since the moving partial tends to reduce its length instead of climbing parallel to its initial direction, the dislocation orientates itself to have the shortest possible length in the climb plane and foil. The details of the climb process (climb plane, further relaxation of both the second partial and the APB, etc.) are still matters of investigation. However, these observations are worthy of mention in the present context since, again, there is a striking difference in behaviour between the two superpartials as if increasing the APB surface were the easiest response of the system to its need to absorb the excess interstitials.

The present irradiation-induced climb experiments were reproducible to such a degree that the change of 7-9nm split dislocations into either dramatically widened planar configurations or helix turns was easily foreseeable. These changes were later used to determine the mixed or screw nature of the dislocation lines respectively. An example of an initially bent segment having undergone both evolutions according to the dislocation character is shown in figure 10.

4.2 Discussion

One of the interesting questions arising from these observations is the reason for the climb asymmetry of the partials. It is likely that the helix turns grow under the same net interstitial flux as that giving rise to the matrix interstitial loops. Therefore, since the two partials have the same character, one expects to observe both of them growing into the same-handed helix. This actually happens with the restriction that when one screw partial climbs, its companion remains hardly affected. During the growth of an helix turn, the increase in line energy is balanced by the energy gain resulting

from the condensation of excess point defects. In $Ni_3Al$, this gain also compensates the increase in surface area of the APB. For the sake of clarity, an helix turn will be regarded as the reaction product of a screw dislocation with an edge loop with the same BV. Under the same interstitial supersaturation, the growth of an imperfect APB loop (b= ½<110>) will be energetically more favorable than a perfect one as long as $2\mu b^2 \pi r + \gamma \pi r^2 < 8 \mu b^2 \pi r$, where the critical radius $r_0$, roughly by $r_0 = 6\mu b^2/\gamma \rightarrow r_0 = 6\mu b^2/\gamma$, characterizes the size below which a loop will remain faulted. Both helix turn and rhombus loop diameters of the order of one micrometer have been observed in the course of irradiation experiments with no clear upper limit since then the defect size is of the order of the foil thickness. This value yields an over-estimate for $\gamma$ of the order of a few $mJ/m^2$, in contradiction to our knowledge of APB energies is $Ni_3Al$ (Veyssière 1984). In the same alloy, the ½<110>{110} climb configurations is rarely observed, but the most favorable {001} glide type and {013} climb one are more common and these have APB energies of the order of 80-100 $mJ/m^2$. Thus, the present investigation points to the formation of faults which are relevant exclusively to irradiation. It is unlikely that the effect could be ascribed to radiation disordering since the irradiation was performed in a temperature range far higher than that at which disordering is known to occur (77-205K) (Liu and Mitchell 1983, Waiting and Butler 1983). Rather, a change in composition of the APB could well explain the dramatic reduction in surface energy, as confirmed by atomistic simulations of non-stoichiometric faults in the $L1_2$ structure (P. Beauchamp, P. Veyssière and J. Douin 1985, unpublished results). In the present case, the situation would be that of an APB where locally, instead of a pair of the Ni and Ni-Al planes of the regular <110> stacking, a plane is inserted in the lattice

with a composition imposed by a net difference in the production or survival rate of Ni or Al interstitials in the crystal. The extreme off-stoichiometric (25% or 75%) (EOS) configurations corresponding to pure Ni or pure Al planes, have not been calculated yet. Direct evidence for the EOS faults on the helix turns was not unambiguously found due to their generally complex configurations. However, other examples of radiation-induced climb dissociation were found exhibiting contrast features which are inconsistent with the stoichiometric condensation of point defects. As shown in the video sequence of Fig. 9, faint residual fringe contrast (King 1966) extends between the two climb-dissociated mixed dislocations as irradiation at 638 °C proceeds. Of the two EOS possibilities, i.e. a double layer of pure Ni or pure Al, the latter would give rise to much larger residual displacements because of its larger mismatch (-1.1% for Ni in $Ni_3Al$ compared with +13.5% for Al). Since numerous weak-beam experiments have resulted in only occasional observations of fringes, we believe the total evidence favours a model in which the Ni EOS fault forms with an APB energy much lower than the lowest stoichiometric case. This may be contrasted with the case of CuAu where interstitial loops of stoichiometric composition are formed (Mukai and Mitchell 1982).

The observations we have made are all consistent with the fact that the edges of the helices produced by irradiation are systematically oriented along well-defined specific crystallographic directions, all of which lie in {111} planes (Table 1). This is entirely consistent with the shape of the APB loops favoured in the matrix, and strongly indicates that a further dissociation of the ½ <110> dislocation segments into two 1/6<112> partials lying in a common {111} plane is occurring. Thus, the rationalisation of the rhombus loop geometry first advanced by Hudson and Makin (1963) and verified in a number of subsequent

studies on Al alloys including the observation of angular helical dislocations in Al-Mg, (K.H. Westmacott 1959, unpublished results) is apparently also valid for $Ni_3Al$.

The equilibrium shape of an edge loop lying on a {110} plane has been calculated using the procedure recently developed by Hazzledine, Karnthaler and Korner (1984); the prediction for the anisotropic elastic constant case appropriate to $Ni_3Al$ is not at all consistent with our experimental findings. However, the calculations are for equilibrium shapes, whereas the present configurations were formed under conditions far from equilibrium.

Although the climb configurations are termed helices, they differ in a number of respects from the regular, symmetrical examples found in quenched metals. First, it is clear that they grow asymmetrically since no intersection with the unclimbed companion is observed. Secondly, growth of the helices occur in two stages. Initially, turns nucleate and grow at widely separated places on the screw dislocation rather than in the uniform manner than would give rise to a continuous smooth helix. At this stage the line segments of a turn are approximately symmetrically oriented relative to the axis as shown in Fig. 11(a) where the mean (110) plane of the turn is shown dashed. During subsequent growth, preferential climb of the B segment occurs to allow both the APB and interstitial plate to lie on the preferred (110) plane (Fig. 11(b)). This must be the case since the turns grew in some instances up to 1μm in extent without intersecting the foil surfaces.

As far as climb of initially mixed segments is concerned, the same argument holds to explain the distinctive behaviour that each superpartial undergoes under irradiation. On the basis of the stress field around the climb split configuration, one would expect interstitials to condense evenly on both partials

since it is unlikely that one of the partials could be a favoured interstitial sink particularly when the initial dissociation width is already 7 to 10 nm; but if one is favoured, the greater their separation after some climb has proceeded, the closer their climb rates should be. Unless some change happens at the APB itself, the correlation motion of the partials is reinforced by the presence of the APB, since their repulsive interaction necessarily balances the constant spring force that the APB exerts on them. Thus, again, the present observations of a dramatic climb asymmetry of the partials having a mixed character supports the idea that the APB energy is significantly lowered by a local compositional change.

## 5. Conclusions

At 750°C, below $V_t$ screw dislocations in $Ni_3Al$ reorient to allow climb dissociation to occur in a more favorable (lower APB energy) plane.

During electron irradiation at 650°C above $V_t$ single superpartial dislocation helices form by the condensation of interstitial atoms. The observed configurations indicate that low energy off-stoichiometric APB's are produced when helix climb is by nickel atom condensation only.

## 6. Acknowledgement

This work is supported by the Director, Office of Energy Research, Office of Basic Energy Sciences, Materials Sciences Division of the U.S. Department of Energy under Contract No. DE-AC03-76SF00098.

We are grateful to J. Douin for preparing the specimens, and to David Ackland for meticulously maintaining the HVEM in optimum working condition and John Turner for the photography.

## 8. REFERENCES


1. Glowinski, L.D., 1976, J. Nucl Mat. 61, 8.
2. Hazzledine, P.M., Karnthaler, H.P., and Korner, A., 1984, Phys. Stat. Sol(a) 81, 473.
3. Huis In't Veld, A. Boom, G. Bronsveld and P.M. De Hosson, J.T.M., 1985, Scripta Metall. 19, 105.
4. Kear, B.H., and Wilsdorf, H.G.F., 1962 Trans. Metall. Soc. A.I.M.E. 224, 382.
5. King, H.W., 1966, J. Mater. Sci., 1, 79.
6. Liu, H.C. and Mitchell, T.E., 1982, Acta metall., 31, 863; 1983, J. Nucl Mater., 107, 318.
7. Makin, M.J. and Hudson, B., 1963, Phil. Mag. 8 , 447.
8. Mukai, T. and Mitchell, T.E., 1982, Phil. Mag. 45, 741.
9. Paidar, 1985, Phys. Stat. Sol.(a), in the press.
10. Paidar, V., Pope, D.P. and Vitek, V., 1984, Acta metall., 32, 43.
11. Pope, D.P. and Ezz, S.S., 1984, Int. Metals Reviews 29, 136.
12. Takeuchi, S., and Kuramoto, E., 1973, Acta metall. 21, 415.
13. Veyssière, P., 1984, Phil. Mag. A., 50, 189.
14. Veyssière, P., Beauchamp, P. and Douin, J., 1985, Phil. Mag. A. 51, 469.
15. Veyssière, P. Guan D. and Rabier, J., 1984, Phil. Mag. A, 49, 45.
16. Yamaguchi, M., Paidar, V., Pope, D.P., and Vitek, V., Phil. Mag. A, 45, 867.
17. Waiting, G.F. and Butler, E.P., 1983, 7$^{th}$ Int. Conf. High Voltage Electron Microscopy, Berkeley, edited by R.M. Fisher, R. Gronsky and K.H. Westmacott (LBL-CONF-830819), p. 307.

TABLE 1

LINE ORIENTATIONS OF DISLOCATION SEGMENTS COMPOSING HELIX TURNS AND POSSIBLE APB PLANES

| | A | | B | | C | | D | | A |
|---|---|---|---|---|---|---|---|---|---|
| line orientation | $[\bar{1}01]$ | | $[112]$ | | $[\bar{1}\bar{1}1]$ | | $\sim[223]$ | | $[\bar{1}01]$ |
| common plane between consecutive segments | | $(1\bar{3}1)$ | | $(1\bar{1}0)$ | | $(1\bar{1}0)$ | | $(2\bar{5}\bar{2})$ | |

## 9. FIGURE CAPTIONS

Figure 1. Sequence of micrographs showing the thermal kinking of initially screw dislocations during in-situ heating at 750°C. The foil plane is (111) and the Burgers vector (BV) of the long screw dislocations lying in the foil are $[1\bar{1}0]$ and $[\bar{1}01]$. The beam direction $\underline{B} = [\bar{1}\bar{1}\bar{1}]$ and diffracting vector $\underline{g} = [2\bar{2}0]$ were maintained constant throughout the experiment. (a) Typical aspect of the dislocation microstructure prior to annealing (sample deformed in compression at 350°C). Note the initially high dislocation density, the regular spacing between dislocations with BV = $[1\bar{1}0]$, and the presence of screw dislocations inclined to the foil with BV = [011] and BV = [110] (out of contrast) (b) Same area after annealing at t = 740°C for a time t = 10 min (accelerating voltage 300 kV). The dislocations have already undergone extensive reorganization. Those with $[1\bar{1}0]$ Burgers vector mostly remain contained within the foil while the others, particularly from the $[\bar{1}01]$ family, have partly disappeared. (c) T = 740°C, t = 86 min: note the amplification of the line instabilities and the presence of dipoles which have narrowed. (d) Semi-weak beam observation at t = 125 min showing that the dislocation width varies along its length depending on the segment orientation. (e) Micrograph taken at room temperature after the annealing sequence was terminated at t = 132 min. The accelerating voltage was increased to 900 kV to optimize the observations. Note the further narrowing of some dipoles.

Figure 2. Examples of configurations analysed by weak-beam stereomicroscopy, (a) Dislocations 1-7 and a-d with BVs $[1\bar{1}0]$ and $[01\bar{1}]$ respectively, having reacted to form a function j with BV = $[10\bar{1}]$, $\underline{B} = [\bar{1}\bar{1}\bar{1}]$. Note the variation of the dissociation width of segments 1 to 4. (b) Same as Figure 2a ($\underline{B} = [\bar{1}10]$) showing that dislocation a-d is dissociated, the dislocation 1-7 is out of

contrast. (c) The dislocation 1-7 is in contrast; under this orientation ($\underline{B}$ = $[\bar{1}\bar{1}0]$), it is clear that segments 1-7 are not dissociated in an unique crystallographic plane. (d) Stereographic projection showing the orientation of the dislocation segments 1-7 with respect to their $[1\bar{1}0]$ BV and to the low temperature and high temperature glide planes (LTGP and HTGP respectively) and {110} glide plane (thick full line). (e) Same as Figure 2d for segments a-d and j.

Figure 3. Another example of a kinked dislocation taken from the same sample as for figure 1. In this case the dislocation has emerged from the surface to only a limited extent. (a) $\underline{B}$ = $[\bar{1}00]$, (b) $\underline{B}$ = $[\bar{1}\bar{1}2]$. Note the pronounced kinked aspect and the variation in dissociation width. (c) Stereographic projection of the dislocation of figure 3a. (d) Stereographic projection of another kinked dislocation similar to that in figure 3a-c, showing the slight differences in the geometrical arrangements of the line with respect to BV, HTGP and LTPG.

Figure 4. Montage showing the effects of electron irradiation at 1500 kV for 11 min. at 627° C (specimen chamber vacuum 3-7 mPa) and subsequent heating to 750°C for 5 min. The images were recorded at 100 kV. Climb of pre-existing screw dislocations into asymmetrical helices has occurred together with the nucleation and growth of Frank and rhombus loops in the matrix. $\underline{B}$ = $[00\bar{1}]$ and $\underline{g}$ = 200.

Figure 5. Transformation of a screw into a helical dislocation during irradiation at 1500 kV and 753°C. (a) t = 0.5 min, (b) t = 1 min, (c) t = 2 min, (d) t = 4 min, (e) t = 5 min, (f) t = 7 min, (g) t = 8 min, (h) t = 9 min (i) t = 10 min.

Figure 6. The initial stages of helix turn growth frozen-in after a few seconds of irradiation at 1500 kV and 650°C by defocussing the beam (Micrographs recorded at 100 kV). The differences in the size of the helix turns along its length is a reflection of the Gaussian profile of the electron beam and resulting variations in dose and climb rates. (a) $\underline{B} = [\bar{1}\bar{1}2]$ showing that the helix turns tend to lie perpendicular to the helix axis. (b) Projection on (011) of the helix turn edges; the unaffected superpartial is clearly visible.

Figure 7. Stereo-photographs of a model showing the topography of the APB resulting from helix formation on only one superpartial.

Figure 8. Video climb sequence on a screw dislocation steeply inclined to the beam showing preferred growth of the segment that keeps the turn on a {110} plane.

Figure 9. Weak beam video sequence showing asymmetrical climb of a mixed segment during irradiation at 1500 kV and 638°C. Note the changes in thickness fringe distribution associated with the motion of the superpartials, and the residual fringe contrast between the dislocations.

Figure 10. Video sequence illustrating the differences in climb behaviour between the mixed and screw portions of the same dislocation.

Figure 11. (a) Initial climb configuration showing symmetrical arrangement of segments about the median (110) plane. (b) subsequent evolution by growth of segment B confines the interstitial plate and the APB to the (110) plane.

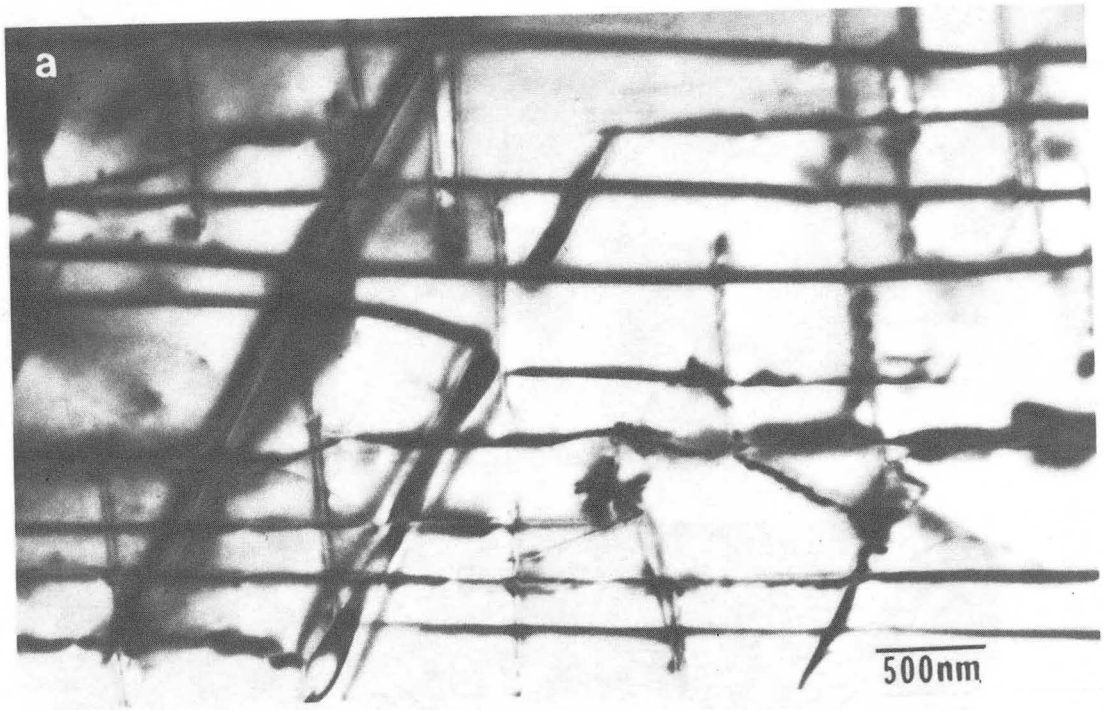


XBB 857-5811

Fig. 1(a)

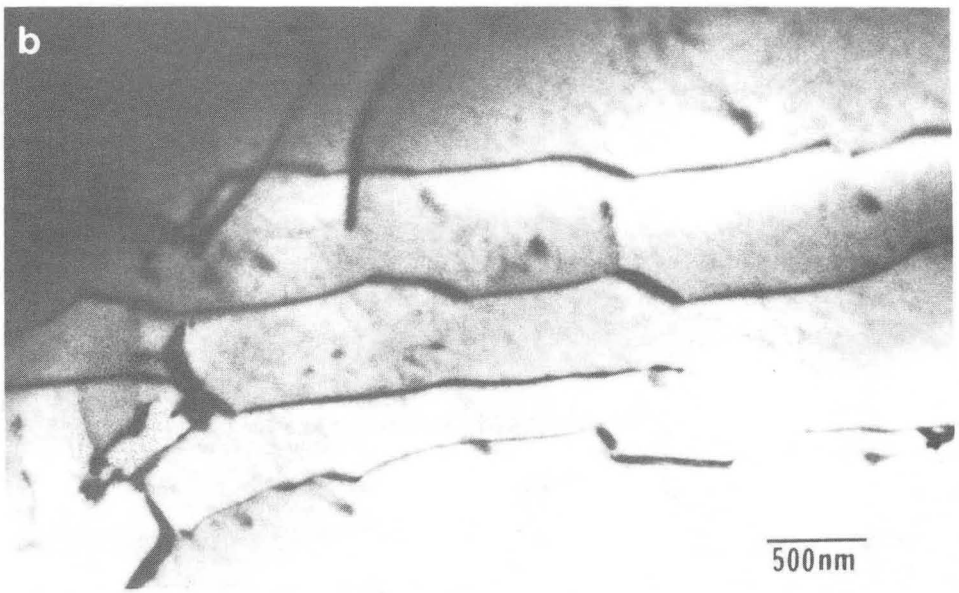


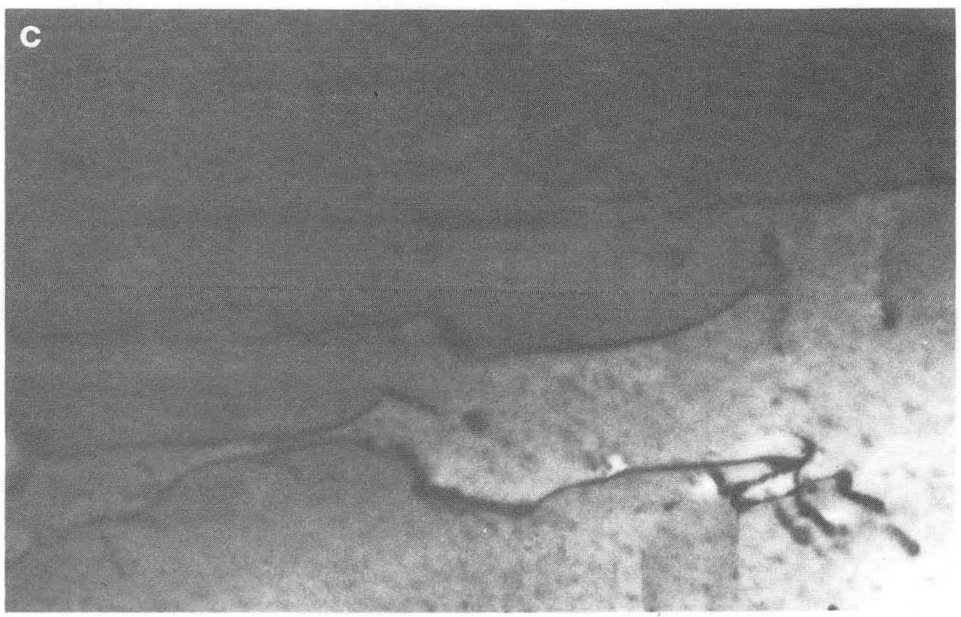


XBB 857-5815

Fig. 1(b,c)

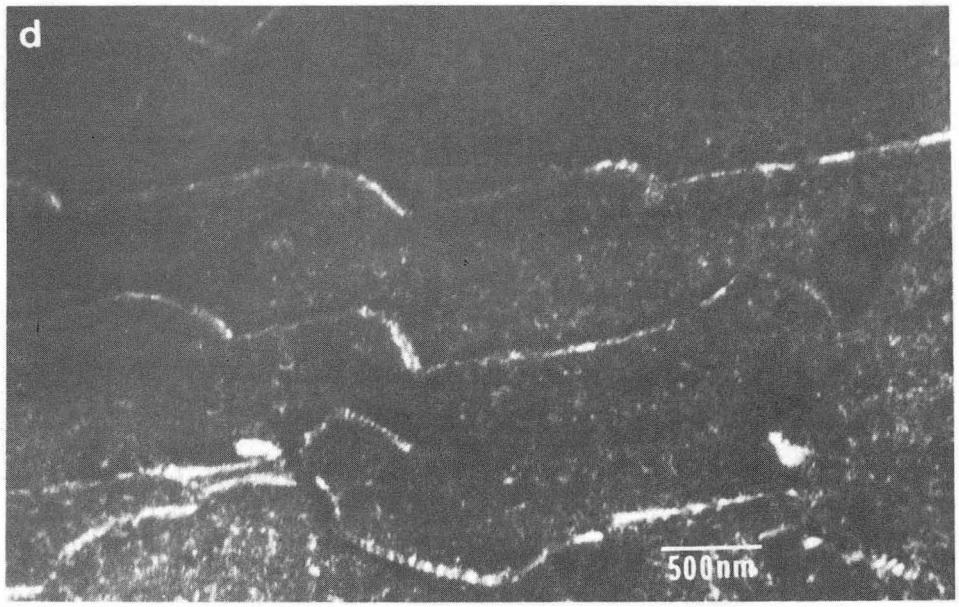


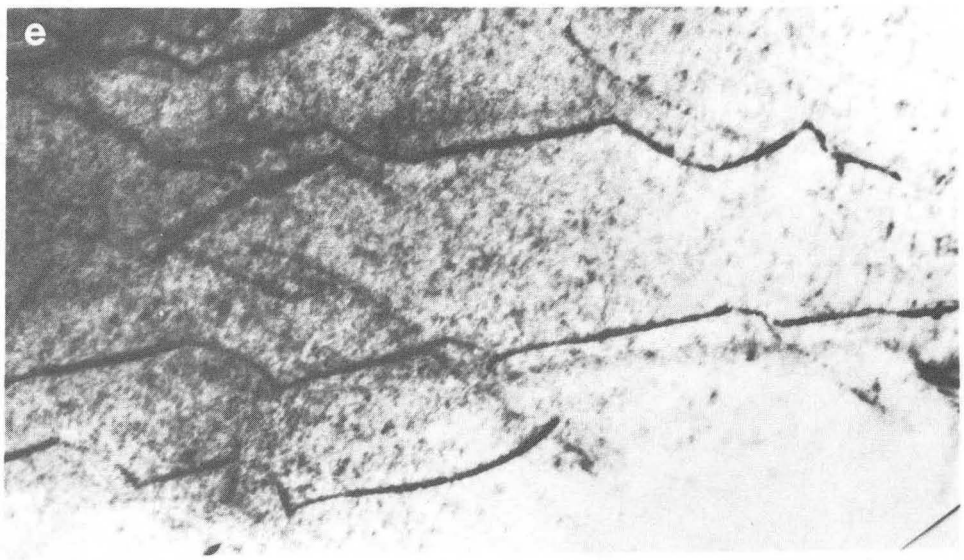


XBB 857-5816

Fig. 1(d,e)

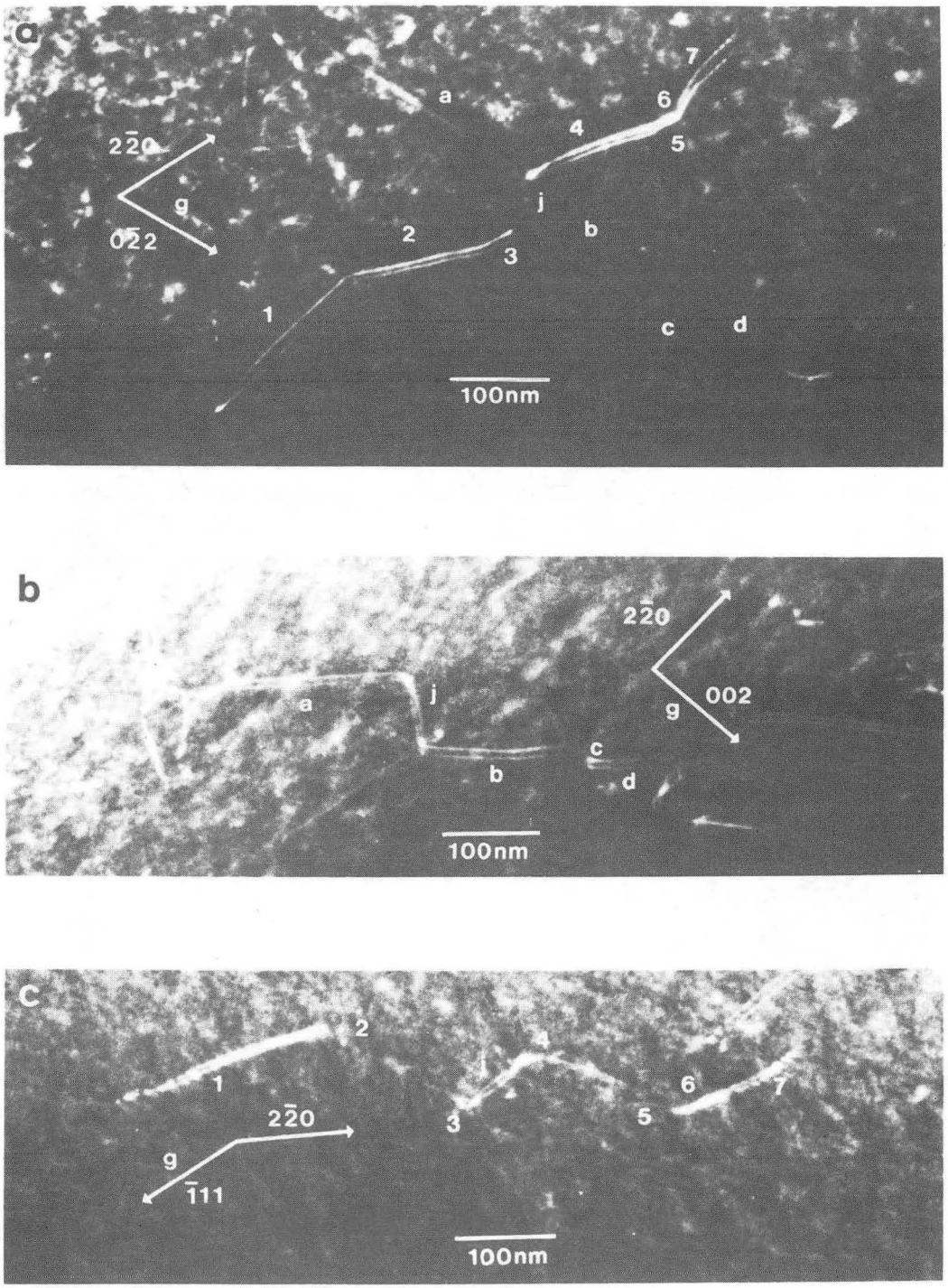


XBB 857-5819

Fig. 2(a,b,c)

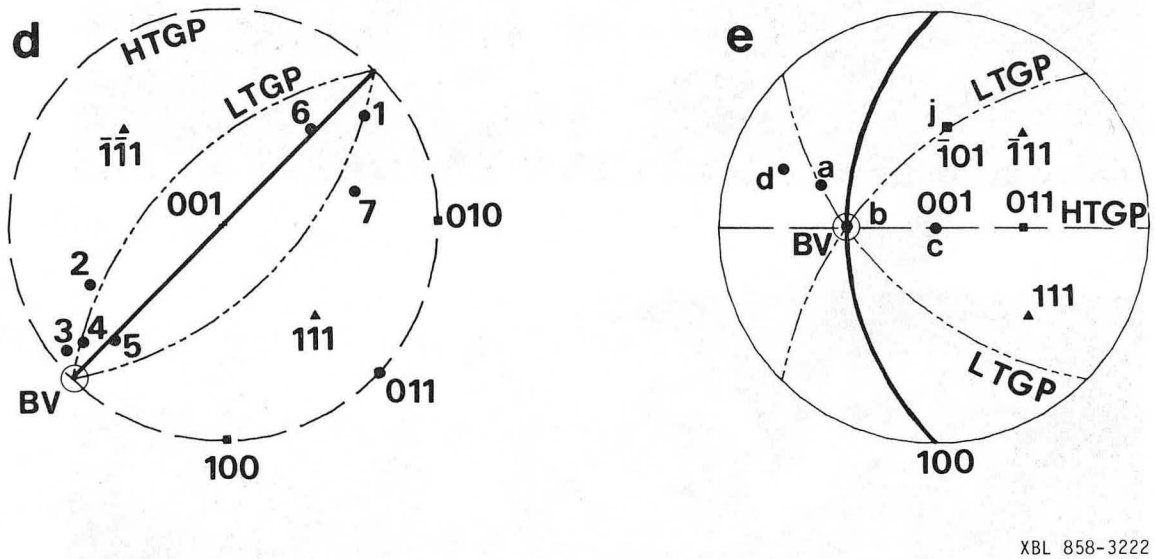
d
HTGP
LTGP
6
1
$\bar{1}\bar{1}1$
001
7
010
2
3
4
5
111
BV
011
100
e
LTGP
j
$\bar{1}01$
$\bar{1}11$
d
a
b
001
011
HTGP
BV
c
111
LTGP
100
XBL 858-3222

Fig. 2(d,e)

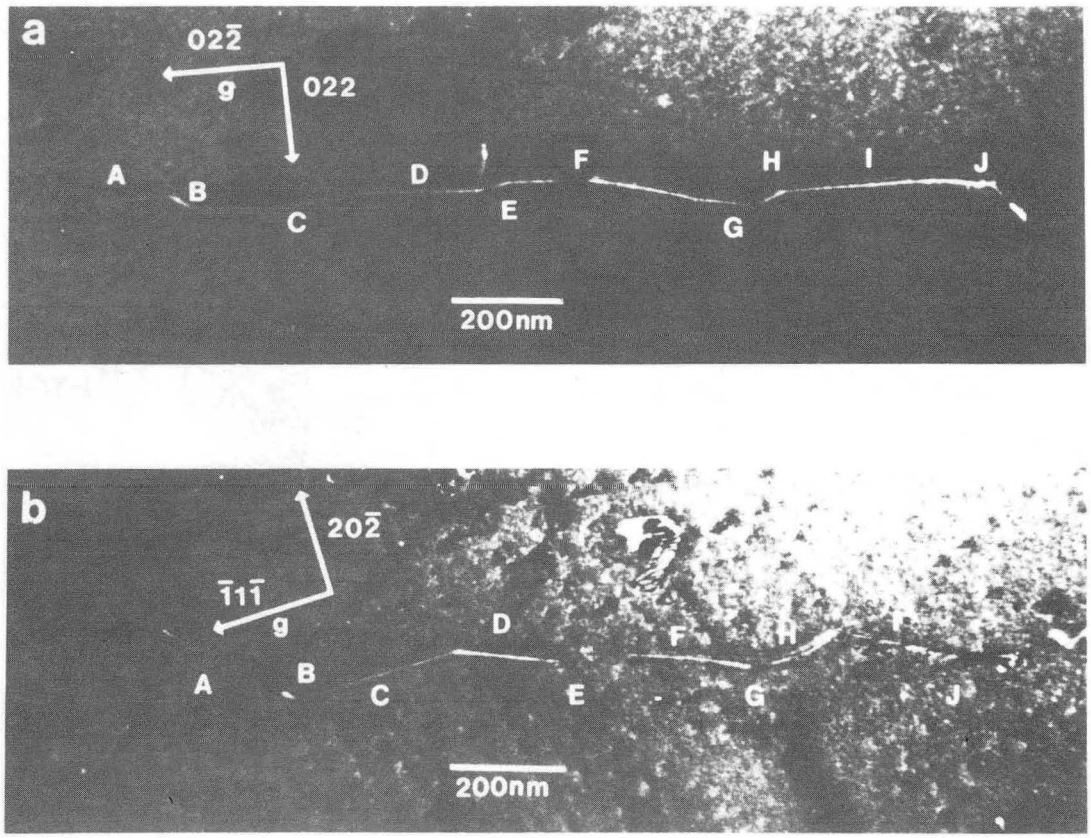


XBB 857-5812

Fig. 3(a,b)

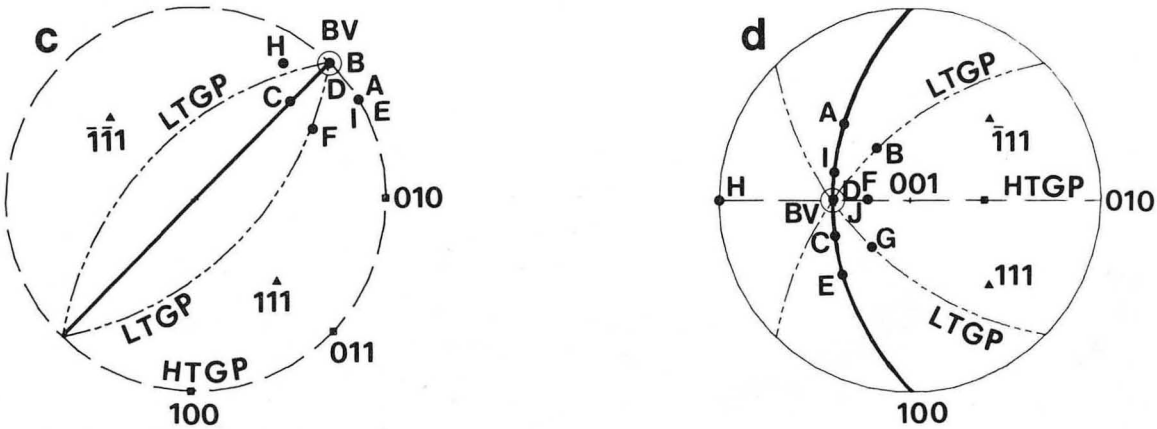


XBL 858-3221

Fig. 3(c,d)

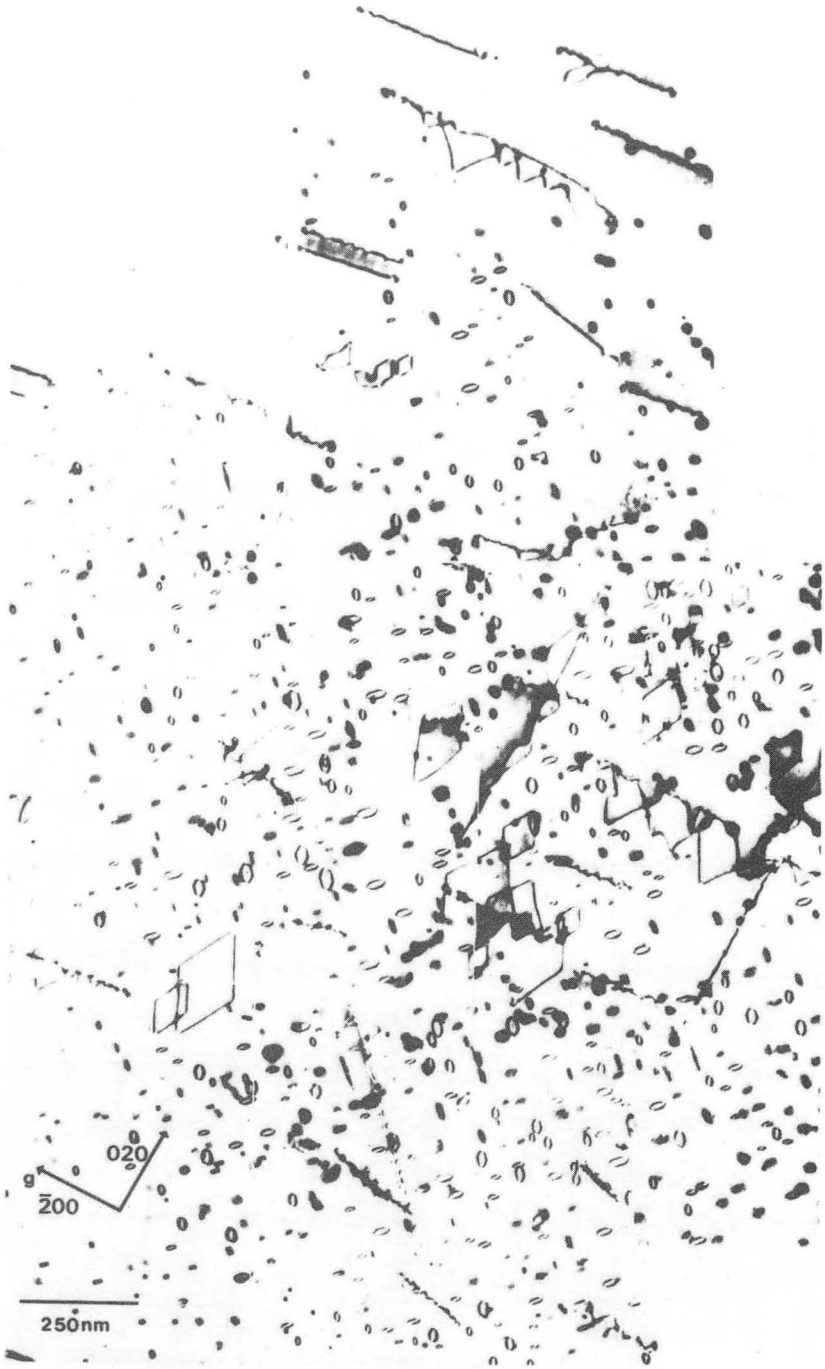


XBB 857-5820

Fig. 4

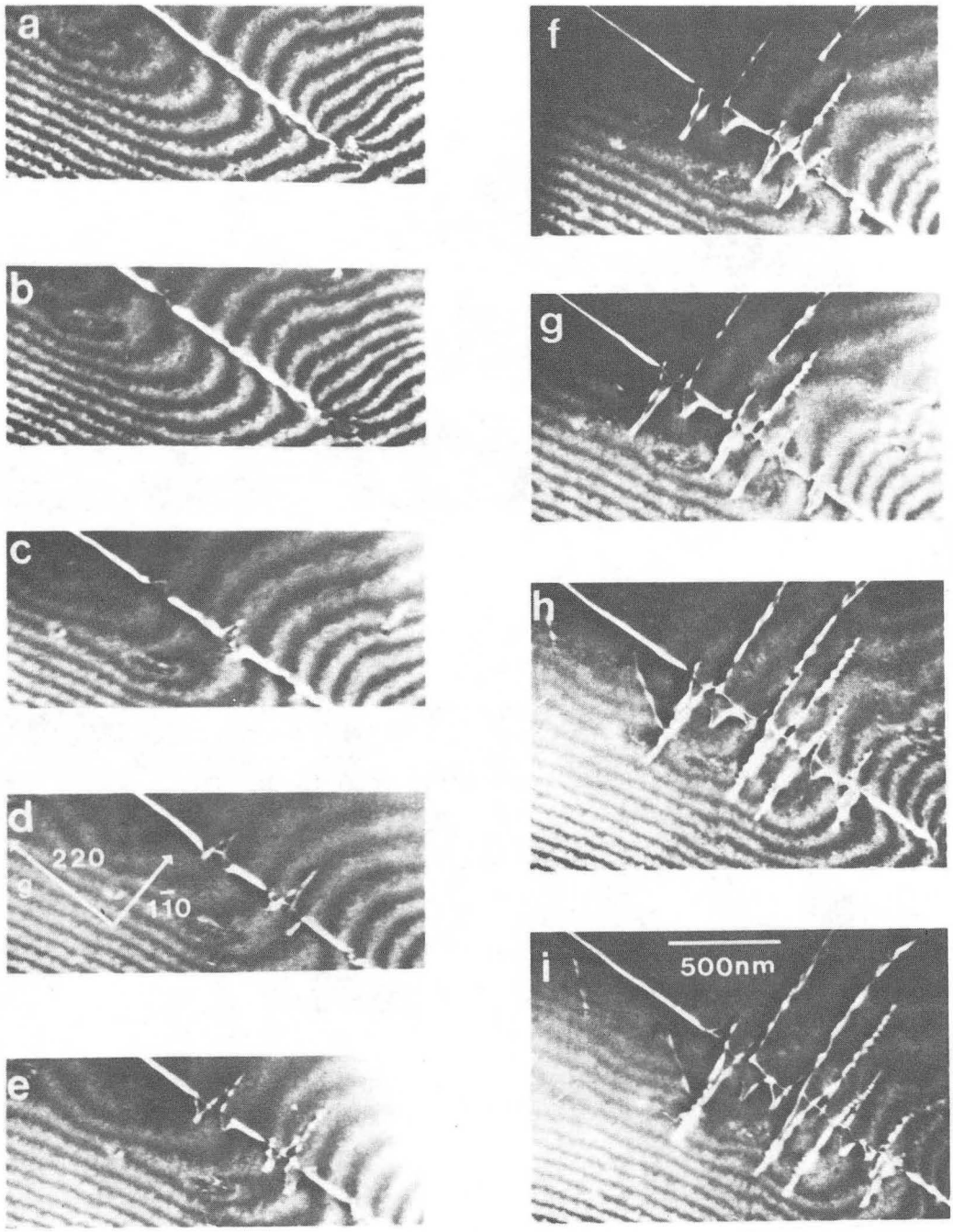


XBB 857-5818

Fig. 5

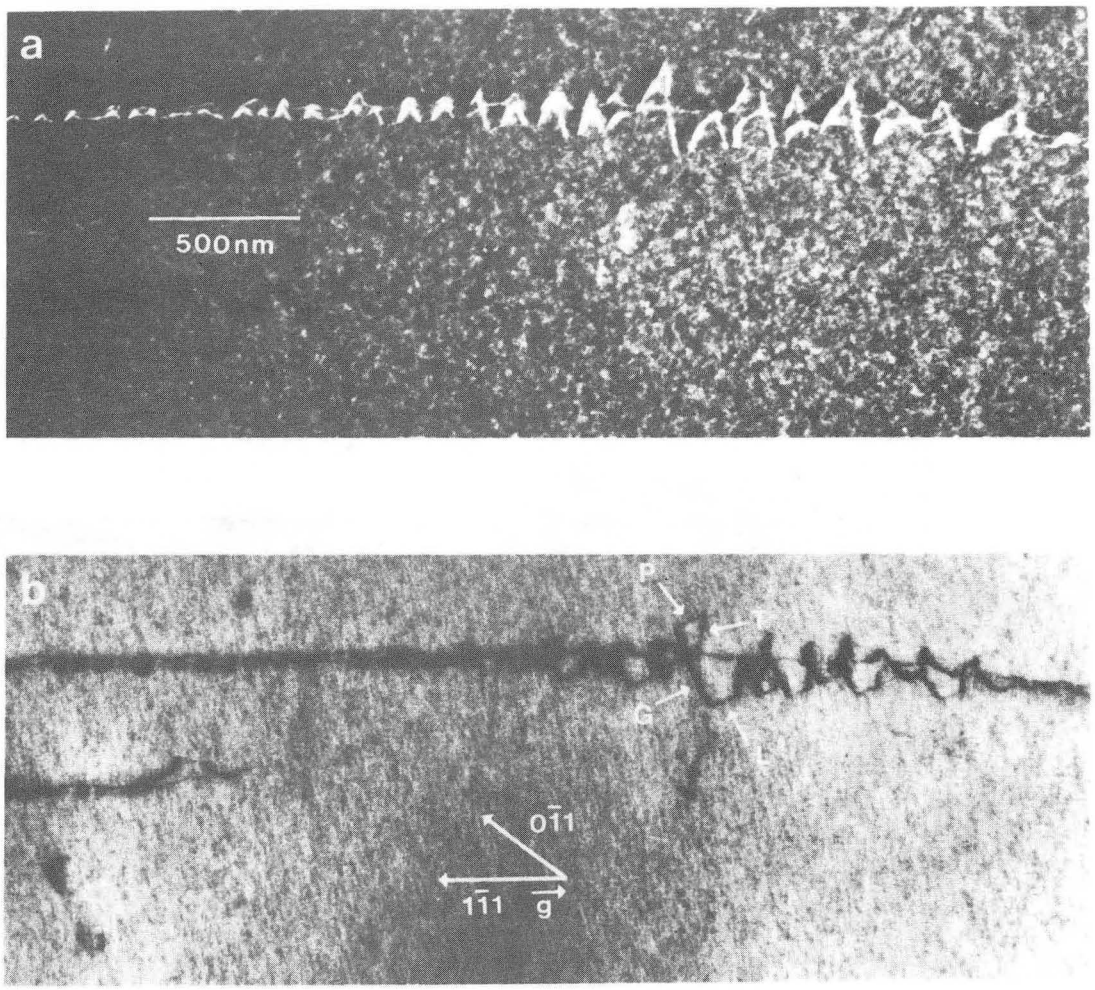


XBB 857-5817

Fig. 6

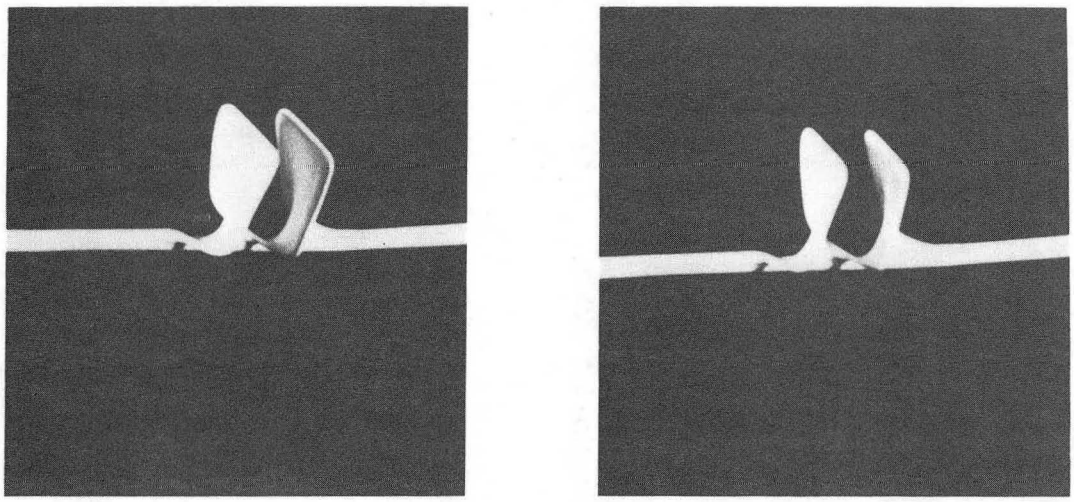

XBB 857-5809

Fig. 7

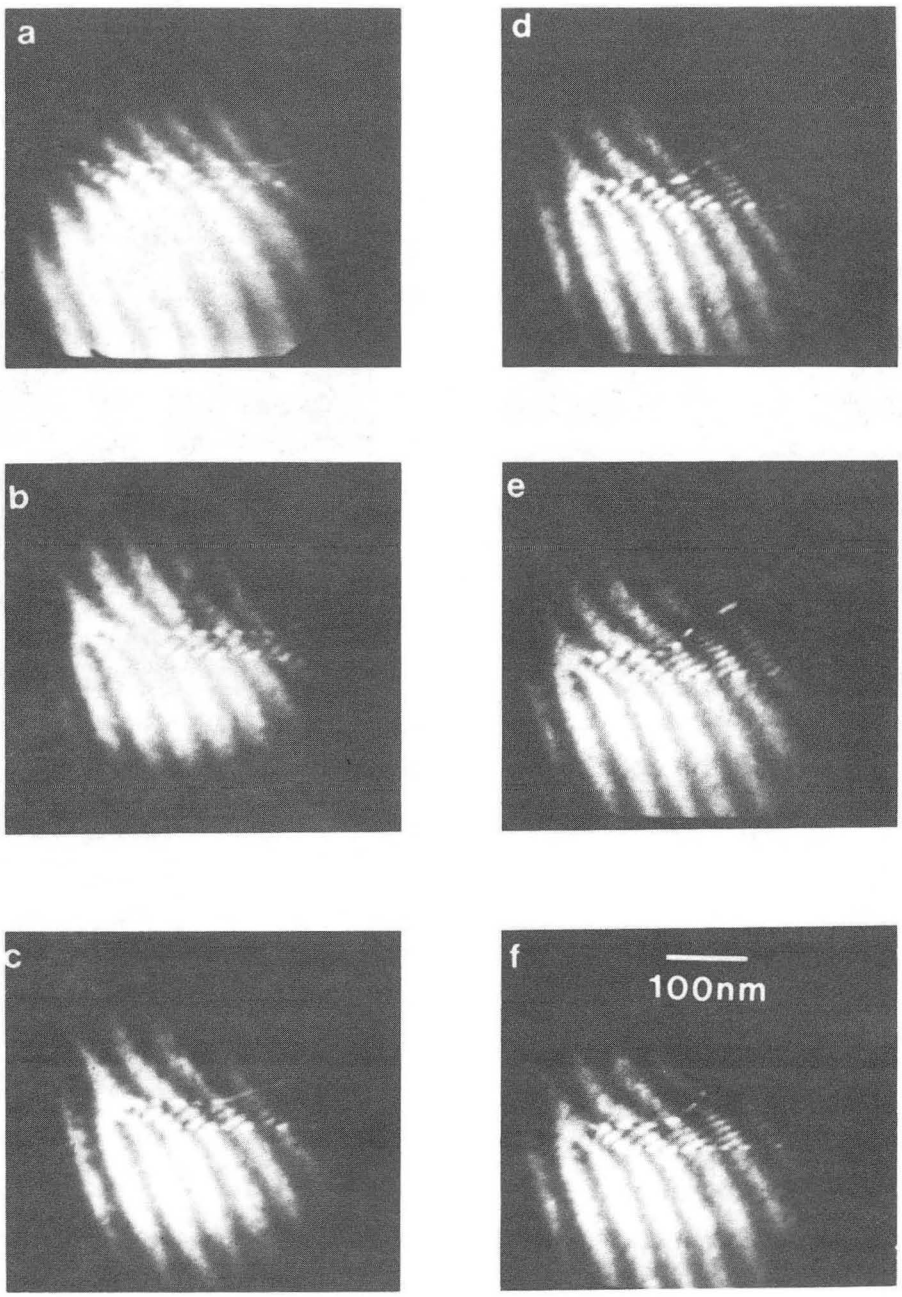


XBB 857-5814

Fig. 8

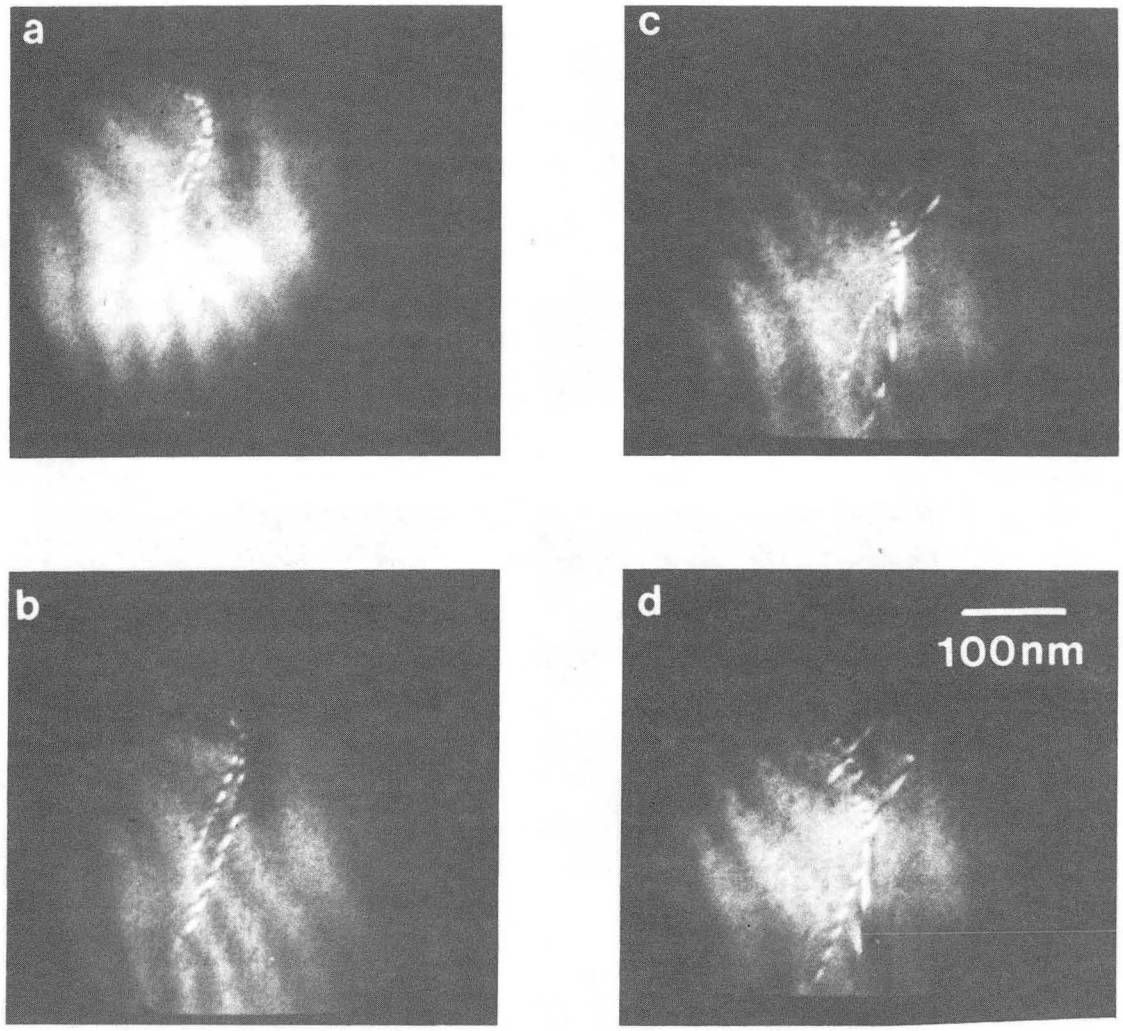


XBB 857-5810

Fig. 9

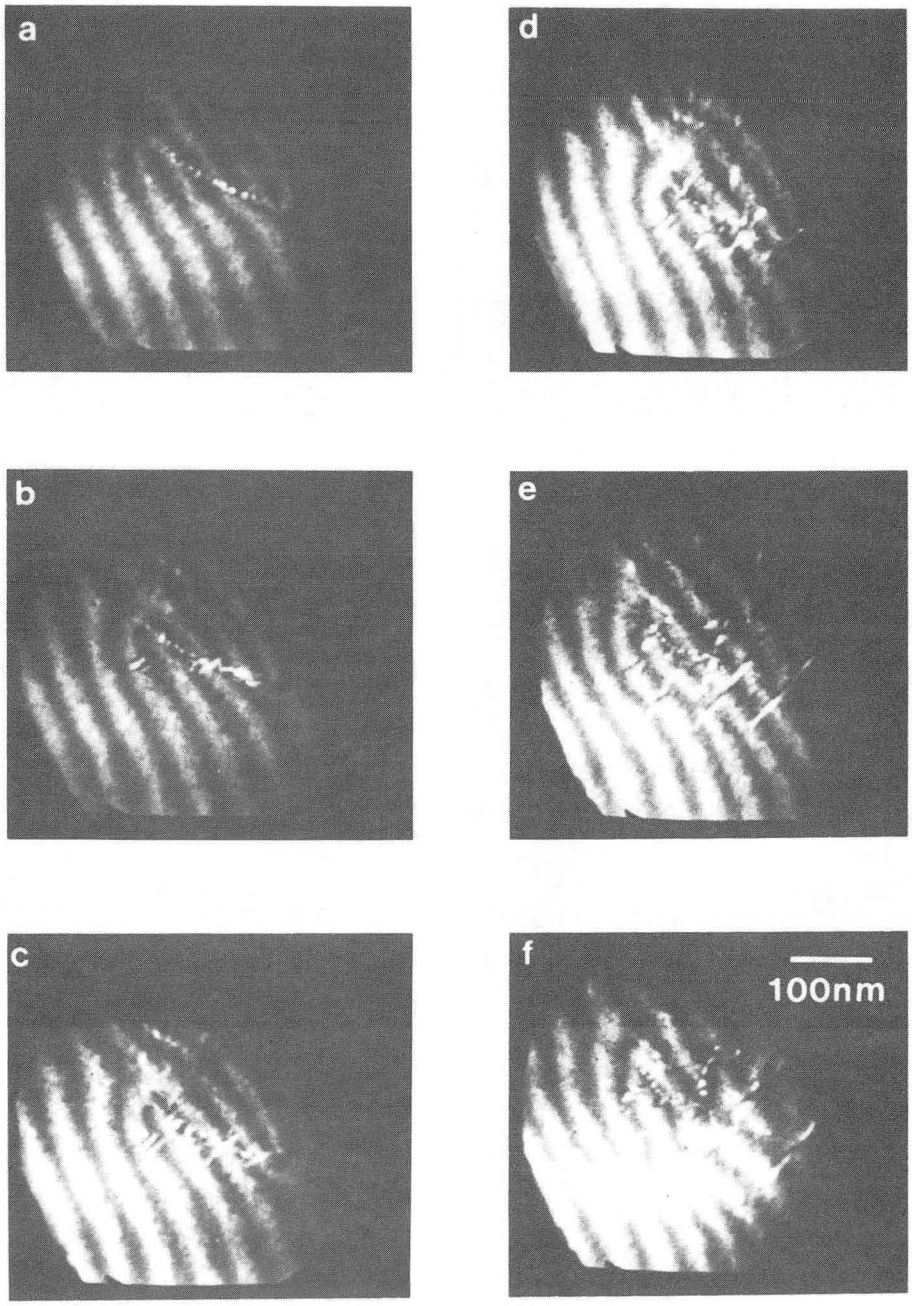


XBB 857-5813

Fig. 10

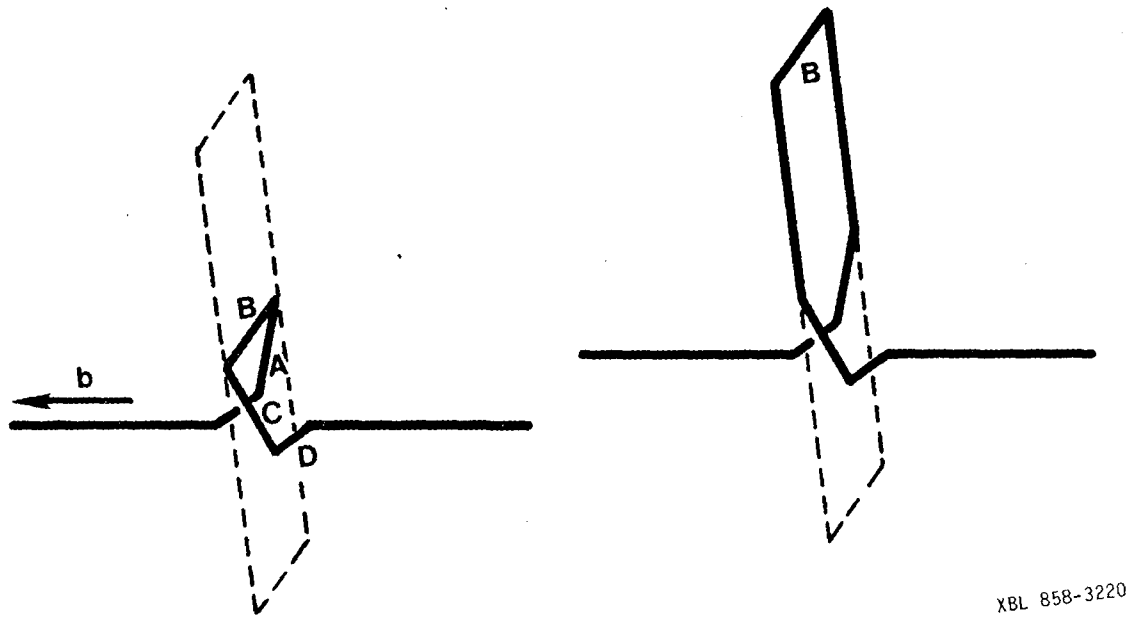


Fig. 11

This report was done with support from the Department of Energy. Any conclusions or opinions expressed in this report represent solely those of the author(s) and not necessarily those of The Regents of the University of California, the Lawrence Berkeley Laboratory or the Department of Energy.

Reference to a company or product name does not imply approval or recommendation of the product by the University of California or the U.S. Department of Energy to the exclusion of others that may be suitable.

*LAWRENCE BERKELEY LABORATORY*
*TECHNICAL INFORMATION DEPARTMENT*
*UNIVERSITY OF CALIFORNIA*
*BERKELEY, CALIFORNIA 94720*